

Fabrication and characterization of perovskite $\text{CH}_3\text{NH}_3\text{Pb}_{1-x}\text{Sb}_x\text{I}_{3-3x}\text{Br}_{3x}$ photovoltaic devices

Jun Yamanouchi, Takeo Oku*, Yuya Ohishi, Misaki Fukaya, Naoki Ueoka,
Hiroki Tanaka and Atsushi Suzuki

Department of Materials Science, The University of Shiga Prefecture,
2500 Hassaka, Hikone, Shiga 522-8533, Japan

(Received May 2, 2018, Revised July 22, 2018, Accepted October 22, 2018)

Abstract. $\text{TiO}_2/\text{CH}_3\text{NH}_3\text{Pb}_{1-x}\text{Sb}_x\text{I}_{3-3x}\text{Br}_{3x}$ -based photovoltaic devices were fabricated by a spin-coating method using mixture solutions with SbBr_3 . Effects of SbBr_3 , CsI or RbBr addition to $\text{CH}_3\text{NH}_3\text{PbI}_3$ precursor solutions on the photovoltaic properties were investigated. The short-circuit current densities and photoconversion efficiencies were improved by adding a small amount of SbBr_3 , CsI or RbBr to the perovskite phase, which would be due to the doping effect of Sb, Br and Cs/Rb atom at the Pb, I and CH_3NH_3 sites, respectively.

Keywords: photovoltaic device; perovskite; SbBr_3 ; microstructure; CsI ; RbBr

1. Introduction

Recently, $\text{CH}_3\text{NH}_3\text{PbI}_3$ perovskite solar cells have been widely studied because they provide higher photoconversion efficiencies than ordinary organic solar cells in a short period of time (Kojima *et al.* 2009, Im *et al.* 2011, Kim *et al.* 2012, Lee *et al.* 2012). Since a conversion efficiency reached 15% (Burschka *et al.* 2013), higher efficiencies than 15% have been achieved for various device structures and processes. The photovoltaic properties of the solar cells depend on the compositions, microstructures and crystal structure of the perovskite compounds. Halogen and metal atom addition such as chlorine (Cl)/bromine (Br), tin (Sn)/antimony (Sb) and cesium (Cs)/rubidium (Rb) at the iodine (I), lead (Pb) and methylammonium (CH_3NH_3) sites in the perovskite compounds have been studied, respectively. Studies on metal atom addition at the Pb sites are interesting from the viewpoint of effects on photovoltaic properties and addition of Sb at the Pb sites has been performed in the previous studies (Oku *et al.* 2016a, b, Zhang *et al.* 2016, Oku *et al.* 2017a). Adding inorganic cation such as Cs or Rb to CH_3NH_3 sites is also interesting from the viewpoint of efficiency improvement and device stability (Saliba *et al.* 2016a, b, Xu *et al.* 2017, Yi *et al.* 2016, Hu *et al.* 2017).

Effects of SbBr_3 addition to $\text{CH}_3\text{NH}_3\text{PbI}_3$ were investigated in the previous work (Oku *et al.* 2017b) and the photoconversion efficiencies were improved by adding 3% SbBr_3 to the perovskite phase. However, further additions of SbBr_3 had not been investigated and other simultaneous

*Corresponding author, Professor, E-mail: oku@mat.usp.ac.jp

additions of compounds such as CsI or RbBr are intriguing to increase the conversion efficiencies. In addition, microstructural and compositional analyses of the perovskite phase had not been performed by X-ray diffraction and scanning electron microscopy with energy dispersive X-ray spectroscopy and further analyses were needed.

The purpose of the present work is to investigate photovoltaic properties of $\text{CH}_3\text{NH}_3\text{PbI}_3$ perovskite solar cells added with SbBr_3 , CsI and RbBr, which were prepared by a simple spin-coating technique in air. The Sb is the group V element and is expected to provide electronic carriers at the sites of the group IV element Pb. Br is a halogen element and is expected to be doped at the sites of the halogen element I. Cs and Rb are also suggested as an added element at the CH_3NH_3 site (Saliba *et al.* 2016a, b, Xu *et al.* 2017, Yi *et al.* 2016, Hu *et al.* 2017). It was also reported that the open circuit voltage was improved by adding a small amount of CsI to $\text{CH}_3\text{NH}_3\text{PbI}_3$ (Ueoka *et al.* 2017). Therefore, the addition of CsI or RbBr to $\text{CH}_3\text{NH}_3\text{Pb}_{1-x}\text{Sb}_x\text{I}_{3-3x}\text{Br}_{3x}$ is expected to increase the open circuit voltages. Effects of SbBr_3 , CsI and RbBr addition into a mixture solution of perovskite compounds on the photovoltaic properties and microstructures were investigated by light-induced current density-voltage (J - V) curves, incident photon-to-current conversion efficiency (IPCE), optical microscopy (OM), X-ray diffraction (XRD) and scanning electron microscopy with energy dispersive X-ray spectroscopy (SEM-EDS).

2. Experimental procedures

A schematic illustration for the fabrication of the present $\text{TiO}_2/\text{CH}_3\text{NH}_3\text{Pb}_{1-x}\text{Sb}_x\text{I}_{3-3x}\text{Br}_{3x}$ -based photovoltaic devices is shown in Fig. 1. The details of the fabrication process are described in the reported papers (Burschka *et al.* 2013, Oku *et al.* 2014, Oku *et al.* 2015, Oku *et al.* 2017b, Oku and Ohishi 2018a, Oku *et al.* 2018b) except for SbBr_3 , CsI and RbBr. F-doped tin oxide (FTO) substrates were cleaned using an ultrasonic bath with acetone and methanol and dried under nitrogen gas. 0.15 and 0.30 M TiO_x precursor solutions were prepared from titanium diisopropoxide bis(acetylacetonate) (Sigma-Aldrich, 0.055 and 0.11 mL) with 1-butanol (1 mL) and the 0.15 M TiO_x precursor solution was spin-coated on the FTO substrate at 3000 rpm for 30 s and annealed at 125°C for 5 min. Then, the 0.30 M TiO_x precursor solution was spin-coated on the TiO_x layer at 3000 rpm for 30 s and annealed at 125°C for 5 min, repeated two times and the FTO substrate was sintered at 500°C for 30 min to form the compact TiO_2 layer. After that, TiO_2 paste was coated on the substrate by spin-coating at 5000 rpm for 30 s. For the formation of mesoporous TiO_2 layer, the TiO_2 paste was prepared with TiO_2 powder (Aerosil, P-25) with poly(ethylene glycol) (Nacalai Tesque, PEG #20000) in ultrapure water. The solution was mixed with acetylacetone (Wako Pure Chemical Industries, 10 μL) and triton X-100 (Sigma-Aldrich, 5 μL) for 30 min and was left for 12 h to suppress the bubbles in the solution. The cells were annealed at 120°C for 5 min and at 500°C for 30 min to form the mesoporous TiO_2 layer. For the preparation of the perovskite compounds, a solution of $\text{CH}_3\text{NH}_3\text{I}$ (Showa Chemical Co., Ltd.), PbI_2 (Sigma-Aldrich), SbBr_3 (Sigma-Aldrich), CsI (Sigma-Aldrich), RbBr (Wako Pure Chemical Industries) and NH_4Cl (Wako Pure Chemical Industries) with a desired mole ratio in a mixed solution of γ -butyrolactone (Nacalai Tesque, 0.3 mL) and N,N -dimethylformamide (Nacalai Tesque, 0.2 mL) was mixed at 60°C. The solution of $\text{CH}_3\text{NH}_3\text{Pb}_{1-x}\text{Sb}_x\text{I}_{3-2x}\text{Br}_{3x}$ -based was then introduced into the TiO_2 mesopores by a spin-coating method and annealed at 100°C for 15 min or 125°C for 20 min. Then, a hole transport layer (HTL) was prepared by spin-coating. As the HTL, a solution of 2,2',7,7'-tetrakis[N,N di(p-methoxyphenyl)amino]-9,9'-spirobifluorene (spiro-OMeTAD, Wako

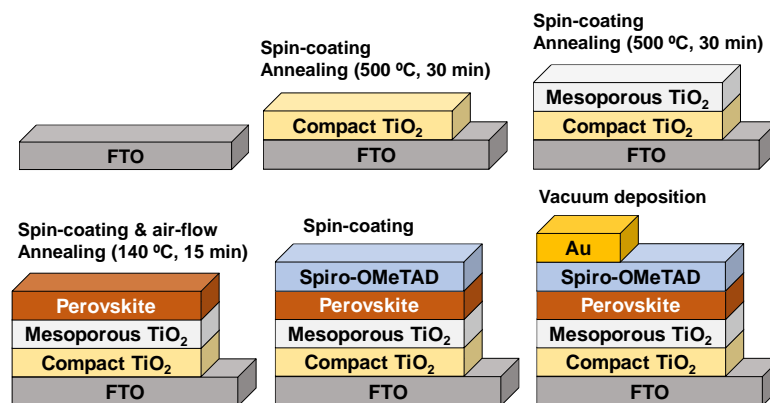


Fig. 1 Schematic illustration for the fabrication process of the present photovoltaic devices

Pure Chemical Industries, 36.1 mg) in chlorobenzene (Wako Pure Chemical Industries, 0.5 mL) was mixed with a solution of lithium bis(trifluoromethylsulfonyl)imide (Li-TFSI, Tokyo Chemical Industry, 260 mg) in acetonitrile (Nacalai Tesque, 0.5 mL) for 12 h. The former solution with 4-tert-butylpyridine (Aldrich, 14.4 μL) was mixed with the Li-TFSI solution (8.8 μL) for 30 min at 70°C. All procedures were carried out in ordinary air. Finally, gold (Au) metal contacts were evaporated as top electrodes. Layered structures of the present photovoltaic cells were denoted as FTO/TiO₂/CH₃NH₃Pb_{1-x}Sb_xI_{3-3x}Br_{3x}-based/spiro-OMeTAD/Au, as shown in a schematic illustration of Fig. 1.

The J - V characteristics (Hokuto Denko HSV-110) of the photovoltaic cells were measured under illumination at 100 mW cm⁻² by using an AM 1.5 solar simulator (San-ei Electric XES-301S). The solar cells were illuminated through the side of the FTO substrates and the illuminated area was 0.090 cm². The IPCE of the cells were also investigated (Enli Technology, QE-R). The microstructures of the thin films were investigated by using SEM-EDS (JEOL JSM-6010PLUS/LA) and an optical microscope (Nikon, Eclipse E600).

3. Results and discussion

Figure 2 is J - V characteristics of the TiO₂/perovskite/spiro-OMeTAD photovoltaic devices under illumination, which indicates effects of SbBr₃, CsI and RbBr addition to the CH₃NH₃PbI₃ phase. The measured photovoltaic parameters of the present devices are summarized as Table 1. The CH₃NH₃PbI₃ (Standard) cell provided a power conversion efficiency (η) of 4.16%, as listed in Table 1.

When SbBr₃ was added to the CH₃NH₃PbI₃ phase, the highest efficiency was obtained for the CH₃NH₃Pb_{0.95}Sb_{0.05}I_{2.85}Br_{0.15} cell (preparation composition), which provided an η of 7.71%, a fill factor (FF) of 0.637, a short-circuit current density (J_{SC}) of 16.30 mA cm⁻² and an open-circuit voltage (V_{OC}) of 0.743 V. In the previous work on SbI₃ addition to the perovskite phase (Oku *et al.* 2016a, b), the photovoltaic cell showed the highest conversion efficiency for Sb 3% addition. The same analogy might be expected in the present work. Actually, in the present work, 3% SbBr₃ and 5% SbBr₃ showed high conversion efficiencies and the conversion efficiencies decreased as the x value (preparation composition of Sb) increased.

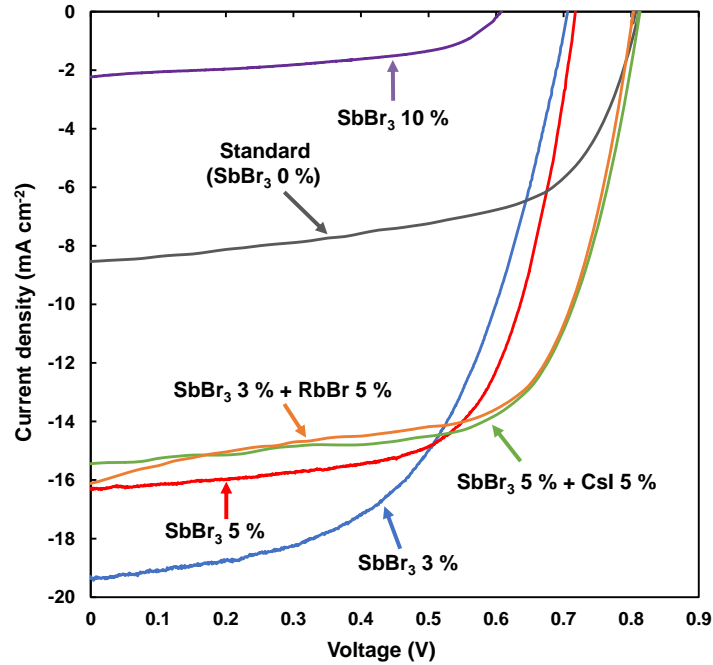
Fig. 2 J - V characteristic of present photovoltaic devices

Table 1 Measured photovoltaic parameters of the present photovoltaic devices

Devices	J_{SC} (mA cm^{-2})	V_{OC} (V)	FF	η (%)
Standard	8.54	0.811	0.602	4.16
SbBr ₃ 3 %	19.40	0.730	0.532	7.52
SbBr ₃ 5 %	16.30	0.743	0.637	7.71
SbBr ₃ 7 %	10.40	0.691	0.644	4.60
SbBr ₃ 10 %	2.23	0.608	0.505	0.68
SbBr ₃ 5 % + CsI 5 %	15.44	0.813	0.667	8.37
SbBr ₃ 3 % + RbBr 5 %	16.12	0.803	0.642	8.30

In addition to the SbBr₃, CsI or RbBr was also added to the perovskite precursor solution. When only SbBr₃ was added, V_{OC} decreased compared with the standard cell. On the other hand, there was no decrease in V_{OC} when CsI or RbBr was added with SbBr₃. SbBr₃ and CsI were also added to the CH₃NH₃PbI₃ phase, the highest efficiency was obtained for the (CH₃NH₃)_{0.95}Cs_{0.05}Pb_{0.95}Sb_{0.05}I_{2.90}Br_{0.15} cell (preparation composition), which provided an η of 8.37%, a FF of 0.667, a J_{SC} of 15.44 mA cm^{-2} and a V_{OC} of 0.813 V.

IPCE spectra of the CH₃NH₃Pb_{1-x}Sb_xI_{3-3x}Br_{3x}-based cells are shown in Fig. 3. The IPCE was improved in the range of 350~740 nm by adding a small amount of SbBr₃, which agrees with J_{SC} values in the J - V characteristics. When CsI or RbBr was added to the CH₃NH₃Pb_{1-x}Sb_xI_{3-3x}Br_{3x}-based cells, no significant change was observed.

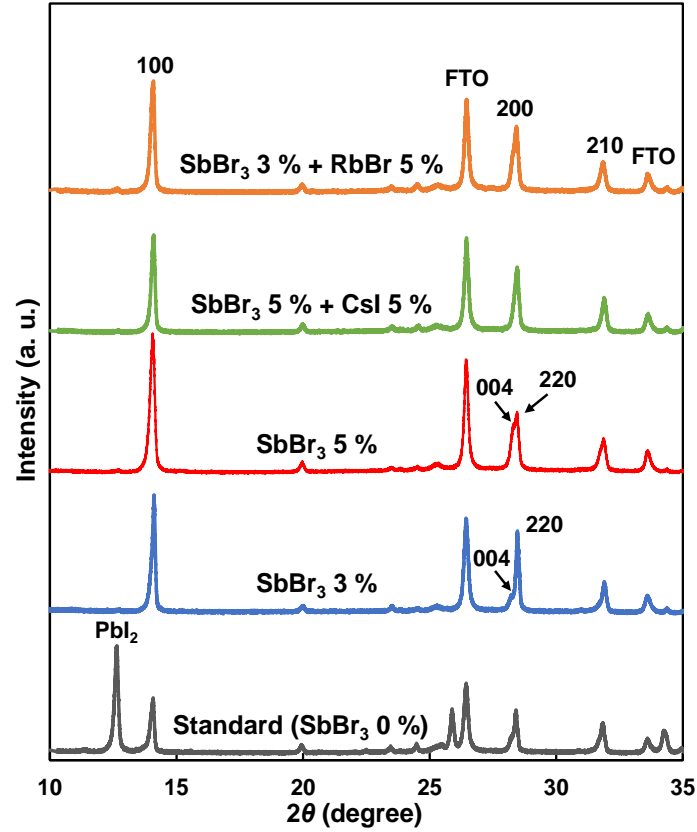


Fig. 4 XRD patterns of the present perovskite photovoltaic devices

XRD patterns of $\text{CH}_3\text{NH}_3\text{Pb}_{1-x}\text{Sb}_x\text{I}_{3-3x}\text{Br}_{3x}$ -based cells on the FTO/ TiO_2 are shown in Fig. 4. All the diffraction peaks can be indexed in a cubic system except for SbBr_3 3% and 5%. The $\text{CH}_3\text{NH}_3\text{Pb}_{0.97}\text{Sb}_{0.03}\text{I}_{2.91}\text{Br}_{0.09}$ and $\text{CH}_3\text{NH}_3\text{Pb}_{0.95}\text{Sb}_{0.05}\text{I}_{2.85}\text{Br}_{0.15}$ (preparation composition) devices showed splitting of 200 peaks, which indicates the formation of tetragonal system. For the standard sample, a strong diffraction peak of PbI_2 is observed, which would be due to the decomposition of $\text{CH}_3\text{NH}_3\text{PbI}_3$. Formation of PbI_2 was suppressed by the SbBr_3 addition.

In each composition, the unit cell volume (V) was calculated from the lattice constants and shown in Table 2. Comparing the V divided by numbers of chemical units in the unit cell (Z), changes of V/Z could be one of experimental evidences of elemental doping. It was confirmed that V/Z decreases due to addition of other elements such as Sb, Br, Cs and Rb. Sb and Br have smaller ionic radii than Pb and I, respectively. Furthermore, Cs and Rb with an ionic radii of 1.67 and 1.52 Å, respectively, which are considerably smaller than that of CH_3NH_3^+ (~2.17 Å) or $(\text{NH}_2)_2\text{CH}^+$ (~2.53 Å) (Hu *et al.* 2017, Duong *et al.* 2016, Saliba *et al.* 2016b, Kieslich *et al.* 2015).

The elemental doping of Sb at the Pb site has been confirmed by using Rietveld refinement in the previous work (Ando *et al.* 2018) and the Sb would be similarly doped at the Pb site in the present work. When CsI was added to $\text{CH}_3\text{NH}_3\text{Pb}_{0.95}\text{Sb}_{0.05}\text{I}_{2.85}\text{Br}_{0.15}$, the V/Z decreases from 247.7 to 246.5 Å³, which indicates the Cs would be doped at the CH_3NH_3 site. In addition, when RbBr

was added to $\text{CH}_3\text{NH}_3\text{Pb}_{0.97}\text{Sb}_{0.03}\text{I}_{2.91}\text{Br}_{0.09}$, the V/Z decreases from 248.0 to 247.6 \AA^3 , which also indicates the Rb would be doped at the CH_3NH_3 site.

Table 2 Measured structural parameters of the present photovoltaic devices. V : unit cell volume. Z : number of chemical units in the unit cell

Devices	Crystal system	Lattice constant (\AA)	V (\AA^3)	Z	V/Z (\AA^3)	I_{100}/I_{210}
Standard	Cubic	$a = 6.284$	248.1	1	248.1	1.87
SbBr ₃ 3%	Tetragonal	$a = 8.860$ $c = 12.63$	991.9	4	248.0	3.98
SbBr ₃ 5%	Tetragonal	$a = 8.868$ $c = 12.60$	990.8	4	247.7	4.22
SbBr ₃ 5% + CsI 5%	Cubic	$a = 6.270$	246.5	1	246.5	3.41
SbBr ₃ 3% + RbBr 5%	Cubic	$a = 6.279$	247.6	1	247.6	3.92

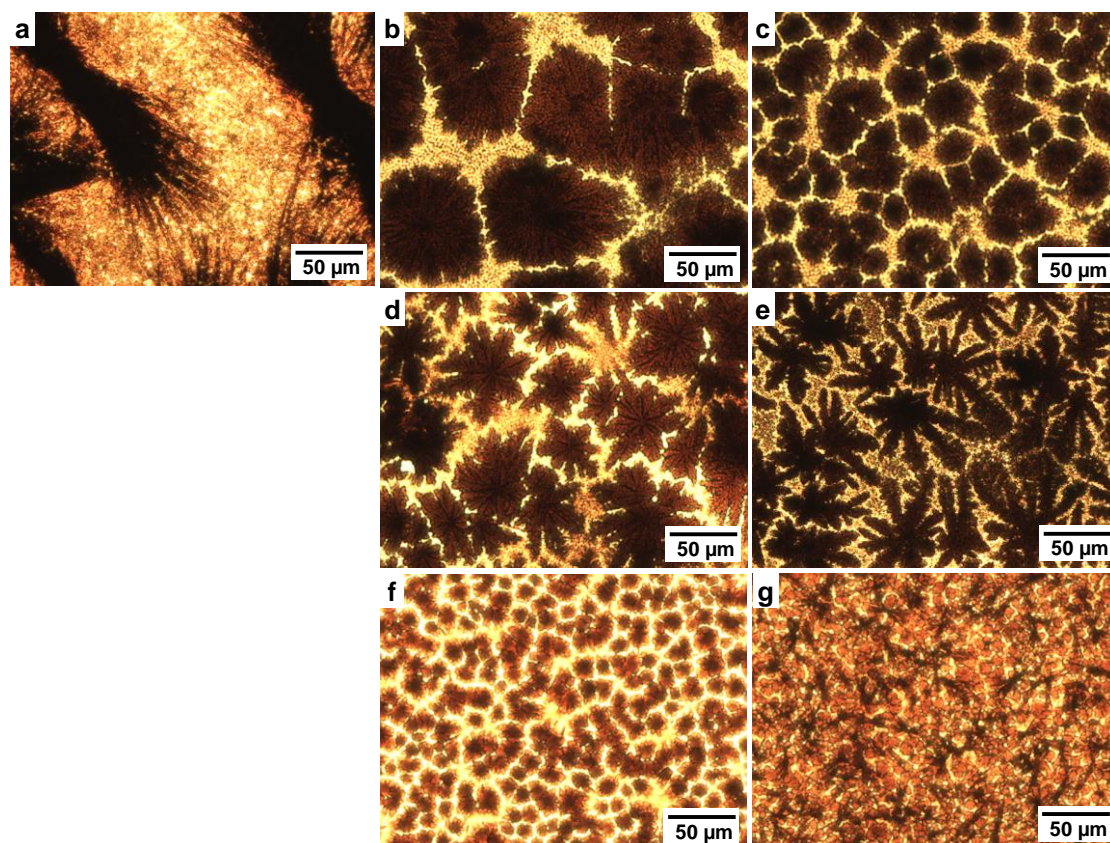


Fig. 5 Optical microscope images of the present devices. (a) Standard $\text{CH}_3\text{NH}_3\text{PbI}_3$, (b) SbBr₃ 3 %, (c) SbBr₃ 5 %, (d) SbBr₃ 7 %, (e) SbBr₃ 10 %, (f) SbBr₃ 5 % + CsI 5 % and (g) SbBr₃ 3 % + RbBr 3 %

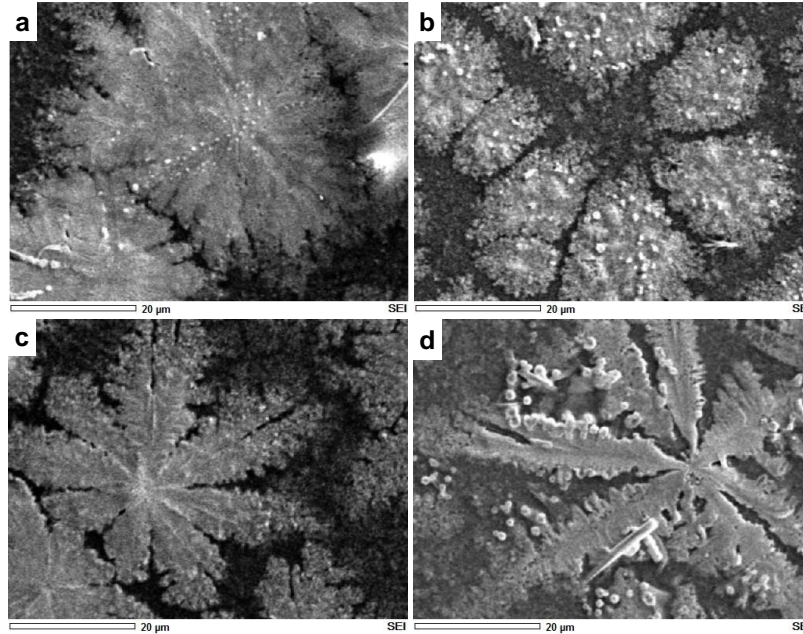


Fig. 6 SEM images of the present devices. (a) SbBr_3 3 %, (b) SbBr_3 5 %, (c) SbBr_3 7 % and (d) SbBr_3 10 %

Table 3 Measured SEM-EDX parameters of the $\text{CH}_3\text{NH}_3\text{Pb}_{1-x}\text{Sb}_x\text{I}_{3-3x}\text{Br}_{3x}$ -based photovoltaic devices

Devices	Pb (%)	Sb (%)	I (%)	Br (%)	Cl (%)	C : N
SbBr_3 3 %	24.7	5.8	62.7	3.0	3.9	55.8 : 44.2
SbBr_3 7 %	21.5	6.8	61.8	6.1	3.8	52.1 : 47.9
SbBr_3 10 %	20.7	9.1	59.4	7.5	3.4	48.9 : 51.1

Therefore, it is considered that the decrease of the lattice constants is due to the incorporation of other elements such as Sb, Br, Cs and Rb into the perovskite crystals. The addition of Cs and Rb is thought to lead to the improvement and stabilization of the surface morphology. (100) preferred orientation was calculated from the ratio of 100 and 210 intensities as I_{100}/I_{210} (Oku *et al.* 2018b). The I_{100}/I_{210} of randomly oriented cubic $\text{CH}_3\text{NH}_3\text{PbI}_3$ crystals was calculated to be 1.79 and the (100) preferred orientation was obtained by the SbBr_3 addition as listed in Table 2.

Optical microscope images of the $\text{CH}_3\text{NH}_3\text{Pb}_{1-x}\text{Sb}_x\text{I}_{3-3x}\text{Br}_{3x}$ -based cells are shown in Fig. 5. The SbBr_3 worked as an accelerator of nucleation growth of perovskite crystals. When the addition of SbBr_3 exceeds 5%, dendrite crystals were formed as shown in Fig. 5(d) and 5(e), which would result in decrease of V_{OC} . When Cs or Rb was added, smaller grains were formed compared with the $\text{CH}_3\text{NH}_3\text{Pb}_{1-x}\text{Sb}_x\text{I}_{3-3x}\text{Br}_{3x}$, as shown in Fig. 5(f) and 5(g). It is considered that the surface morphology was improved by homogenization of the perovskite grains, which would result in the improvement of V_{OC} of the $\text{CH}_3\text{NH}_3\text{Pb}_{1-x}\text{Sb}_x\text{I}_{3-3x}\text{Br}_{3x}$.

Figure 6 are SEM images of $\text{TiO}_2/\text{CH}_3\text{NH}_3\text{Pb}_{1-x}\text{Sb}_x\text{I}_{3-3x}\text{Br}_{3x}$ -based devices, which corresponds to the optical microscope image of Fig. 5. Depending on the amount of SbBr_3 added to $\text{CH}_3\text{NH}_3\text{PbI}_3$, the surface morphology changed drastically, which agrees well with those observed

in the optical microscope image of Fig. 5.

The composition ratio of metal elements Pb, Sb, I, Br, Cl and C-N were measured from the EDX spectra using background correction by normalizing the spectrum peaks on the atomic concentration, as listed in Table 3. Chlorine is derived from NH_4Cl added to perovskite precursor solution and the composition of Sb and Br increased in proportion to the addition amount of SbBr_3 .

Other electronic properties of the thin films are also important to understand the mechanism in detail and further studies are necessary for the future work. The overall cell performances were not good and unfortunately, statistic data were not obtained in the present work. Further optimization is also required even for the standard cell.

4. Conclusion

$\text{TiO}_2/\text{CH}_3\text{NH}_3\text{Pb}_{1-x}\text{Sb}_x\text{I}_{3-2x}\text{Br}_{3x}$ -based photovoltaic devices were fabricated by a spin-coating method in air. The effects of SbBr_3 , CsI and RbBr addition to the $\text{CH}_3\text{NH}_3\text{PbI}_3$ precursor solutions on the photovoltaic properties were investigated. The short-circuit current densities and IPCE values in the range of 350~740 nm were improved by adding a small amount of SbBr_3 to the perovskite phase, which resulted in the increase of photoconversion efficiencies. This improvement would be due to the doping effect of Sb or Br atoms at the Pb or I sites. The decrease in open-circuit voltage due to addition of SbBr_3 was suppressed by further adding a small amount of CsI or RbBr to the perovskite phase. This suppression would be due to improvement of the surface morphology and coverage caused by doping of Cs or Rb atoms at the CH_3NH_3 site.

Acknowledgments

This work was partly supported by Satellite Cluster Program of the Japan Science and Technology Agency.

References

- Ando, Y., Oku, T. and Ohishi, Y. (2018), "Rietveld refinement of crystal structure of perovskite $\text{CH}_3\text{NH}_3\text{Pb}(\text{Sb})\text{I}_3$ solar cells", *Jpn. J. Appl. Phys.*, **57**(2S2), 1-5.
- Burschka, J., Pellet, N., Moon, S.J., Humphry-Baker, R., Gao, P., Nazeeruddin, M.K. and Grätzel, M. (2013), "Sequential deposition as a route to high-performance perovskite-sensitized solar cells", *Nature*, **499**(7458), 316-319.
- Duong, T., Mulmudi, H.K., Shen, H., Wu, Y., Barugkin, C., Mayon, Y.O., Nguyen, H.T., Macdonald, D., Peng, J., Lockrey, M., Li, W., Cheng, Y., White, T.P., Weber, K. and Catchpole, K. (2016), "Structural engineering using rubidium iodide as a dopant under excess lead iodide conditions for high efficiency and stable perovskites", *Nano Energy*, **30**, 330-340.
- Hu, Y., Aygüler, M.F., Petrus, M.L., Bein, T. and Docampo, P. (2017), "Impact of rubidium and cesium cations on the moisture stability of multiple-cation mixed-halide perovskites", *ACS Energy Lett.*, **2**(10), 2212-2218.
- Im, J.H., Lee, C.R., Lee, J.W., Park, S.W. and Park, N.G. (2011), "6.5% efficient perovskite quantum-dot-sensitized solar cell", *Nanoscale*, **3**(10), 4088-4093.
- Kieslich, G., Sun, S. and Cheetham, A.K. (2015), "An extended tolerance factor approach for organic-inorganic perovskites", *Chem. Sci.*, **6**(6), 3430-3433.
- Kim, H.S., Lee, C.R., Im, J.H., Lee, K.B., Moehl, T., Marchioro, A., Moon, S.J., Humphry-Baker, R., Yum,

- J.H., Moser, J.E., Grätzel, M. and Park, N.G. (2012), "Lead iodide perovskite sensitized all-solid-state submicron thin film mesoscopic solar cell with efficiency exceeding 9%", *Sci. Rep.*, **2**, 591.
- Kojima, A., Teshima, K., Shirai, Y. and Miyasaka, T. (2009), "Organometal halide perovskites as visible-light sensitizers for photovoltaic cells", *J. Am. Chem. Soc.*, **131**(17), 6050-6051.
- Lee, M.M., Teuscher, J., Miyasaka, T., Murakami, T.N. and Snaith, H.J. (2012), "Efficient hybrid solar cells based on meso-superstructured organometal halide perovskites", *Science*, **338**(6107), 643-647.
- Oku, T., Zushi, M., Imanishi, Y., Suzuki, A. and Suzuki, K. (2014), "Microstructures and photovoltaic properties of perovskite-type $\text{CH}_3\text{NH}_3\text{PbI}_3$ compounds", *Appl. Phys. Express*, **7**(12), 121601.
- Oku, T., Iwata, T. and Suzuki, A. (2015), "Effects of niobium addition into TiO_2 layers on $\text{CH}_3\text{NH}_3\text{PbI}_3$ -based photovoltaic devices", *Chem. Lett.*, **44**(7), 1033-1035.
- Oku, T., Ohishi, Y. and Suzuki, A. (2016a), "Effects of antimony addition to perovskite-type $\text{CH}_3\text{NH}_3\text{PbI}_3$ photovoltaic devices", *Chem. Lett.*, **45**(2), 134-136.
- Oku, T., Ohishi, Y., Suzuki, A. and Miyazawa, Y. (2016b), "Effects of Cl addition to Sb-doped perovskite-type $\text{CH}_3\text{NH}_3\text{PbI}_3$ photovoltaic devices", *Metals*, **6**(7), 147.
- Oku, T., Ohishi, Y. and Suzuki, A. (2017a), "Effects of NH_4Cl addition to perovskite $\text{CH}_3\text{NH}_3\text{PbI}_3$ photovoltaic devices", *J. Ceram. Soc. Jpn.*, **125**(4), 303-307.
- Oku, T., Ohishi, Y. and Suzuki, A. (2017b), "Effects of SbBr_3 addition to $\text{CH}_3\text{NH}_3\text{PbI}_3$ ", *AIP Conf. Proc.*, **1807**(1).
- Oku, T. and Ohishi, Y. (2018a), "Effects of annealing on $\text{CH}_3\text{NH}_3\text{PbI}_3(\text{Cl})$ perovskite photovoltaic devices", *J. Ceram. Soc. Jpn.*, **126**(1), 56-60.
- Oku, T., Ohishi, Y. and Ueoka, N. (2018b), "Highly (100)-oriented $\text{CH}_3\text{NH}_3\text{PbI}_3(\text{Cl})$ perovskite solar cells prepared with NH_4Cl using an air blow method", *RSC Advances*, **8**(19), 10389-10395.
- Saliba, M., Matsui, T., Domanski, K., Seo, J.Y., Ummadisingu, A., Zakeeruddin, S.M., Correa-Baena, J.P., Tress, W.R., Abate, A., Hagfeldt, A. and Grätzel, M. (2016a), "Incorporation of rubidium cations into perovskite solar cells improves photovoltaic performance", *Science*, **354**(6304), 206-209.
- Saliba, M., Matsui, T., Seo, J.Y., Domanski, K., Correa-Baena, J.P., Nazeeruddin, M.K., Zakeeruddin, S.M., Tress, W., Abate, A., Hagfeldt, A. and Grätzel, M. (2016b), "Cesium-containing triple cation perovskite solar cells: Improved stability, reproducibility and high efficiency", *Energy Environ. Sci.*, **9**(6), 1989-1997.
- Ueoka, N., Ohishi, Y., Shirahata, Y., Suzuki, A. and Oku, T. (2017), "Fabrication and characterization of $\text{CH}_3\text{NH}_3(\text{Cs})\text{Pb}(\text{Sn})\text{I}_3(\text{Br})$ perovskite solar cells", *AIP Conf. Proc.*, **1807**(1).
- Xu, F., Zhang, T., Li, G. and Zhao, Y. (2017), "Mixed cation hybrid lead halide perovskites with enhanced performance and stability", *J. Mater. Chem. A*, **5**(23), 11450-11461.
- Yi, C., Luo, J., Meloni, S., Boziki, A., Ashari-Astani, N., Grätzel, C., Zakeeruddin, S.M., Röhrlisberger, U. and Grätzel, M. (2016), "Entropic stabilization of mixed A-cation ABX_3 metal halide perovskites for high performance perovskite solar cells", *Energy Environ. Sci.*, **9**(2), 656-662.
- Zhang, J., Shang, M.H., Wang, P., Huang, X., Xu, J., Hu, Z., Zhu, Y. and Han, L. (2016), "n-type doping and energy states tuning in $\text{CH}_3\text{NH}_3\text{Pb}_{1-x}\text{Sb}_{2x/3}\text{I}_3$ perovskite solar cells", *ACS Energy Lett.*, **1**(3), 535-541.

